PREDICTED FAR FIELD RESPONSE OF QUASI-ISOTROPIC LAMINATES TO INTERNAL IMPULSIVE EVENTS

E. Rhian Green
Department of Engineering
Leicester University
Leicester LE1 7RH, U.K.

W. A. Green
Department of Mathematical Sciences
Loughborough University
Loughborough LE11 3TU, U.K.

INTRODUCTION

The near field dynamic response of a quasi-isotropic laminate to a number of impulsive internal line sources has been considered in the companion paper [1]. That paper deals with three different line dislocation sources located at each of the seven ply interfaces in turn and shows the time histories of the top surface normal displacement at a distance of one plate thickness from the vertical plane containing the line of action of the source. In this paper attention is focussed on the far field disturbances arising from a line dislocation in the form of a step function in time and corresponding to a crack opening displacement discontinuity acting at each of the seven interfaces in turn. The time history of the normal displacement at the upper surface is presented for receivers located at a distance of 20 plate thicknesses from the plane of action of the sources.

The method of solution involves evaluating the contributions to the displacement arising from a total of twenty branches of the dispersion equation for the modes of propagation of straight crested (Rayleigh-Lamb) waves in the laminate. Curves are presented showing the contributions arising from some of the individual branches of the Rayleigh-Lamb equation for each of the different source locations. The modes of propagation vary with the orientation of the wave front relative to some specified direction, which is here taken to be the fiber direction in the outer layers of the laminate. The results displayed are for waves travelling along this fiber direction and for waves travelling at right angles to this direction. For waves travelling at right angles to the surface fibers, the source at the interface between the top layer and the next, gives rise to a strong Rayleigh wave component in the response

Review of Progress in Quantitative Nondestructive Evaluation, Vol. 18
Edited by Thompson and Chimenti, Kluwer Academic/Plenum Publishers, 1999

which arises from the short wave limiting behaviour of the fundamental mode. For waves travelling along the fiber direction and initiated by a source in the same location, no such large amplitude Rayleigh disturbance is to be seen and the major contribution to the response comes from the seventh mode of the Rayleigh-Lamb equation.

THEORY

The plate is constructed from eight layers each of depth h of a unidirectional fiber reinforced material arranged in a symmetric quasi-isotropic configuration, $(0, \pm 45, 90)_s$ Each layer is modelled as a transversely isotropic elastic continuum, with the axis of transverse isotropy being parallel to the fiber direction. This paper is concerned with straight crested waves travelling in the plane of the laminate and a Cartesian coordinate system of axes $Ox_1x_2x_3$ is chosen, with the origin O in the mid-plane of the plate and Ox_1 in the direction normal to the plate. Ox_2 is parallel to the fibers in the two core layers and Ox_3 is parallel to the fibers in the two outer layers. Attention is restricted to line sources either parallel to Ox_2 or parallel to Ox_3, which initiate waves travelling along Ox_3 and Ox_2, respectively. The governing equations then involve functions of two spatial coordinates x_1 and x (where x may be either of x_2 or x_3) and of the time t. The equations of motion within each layer are reduced to a system of six first order differential equations by taking the Fourier transform with respect to x and the Laplace transform with respect to t as outlined in Green [2]. The solution within each layer is given in terms of six arbitrary constants and imposing the conditions across the interfaces, together with the boundary conditions, leads to a system of 48 linear simultaneous equations for the 48 arbitrary constants. This system can be reduced to two separate systems of 24 equations by rewriting the problem as the sum of a symmetric and an antisymmetric loading problem. Each of these systems has the form

$$M(k,s)K = G(s), \tag{1}$$

where $M(k,s)$ is a square matrix of order 24, K is the column vector of arbitrary constants and $G(s)$ is a column vector whose components arise from the discontinuities acting across the interfaces. The matrix M in equation (1) is a function of the elastic constants, the material density, as well as of the Fourier transform parameter k and the Laplace transform parameter s. The solution of equations (1) may be written in the form

$$K = M^{-1}(k,s)G(s) = \frac{adjM(k,s)}{detM(k,s)}G(s), \tag{2}$$

where $adjM$ is the adjoint matrix of M and $detM$ is the determinant of M.

The transforms of the displacement and stress components at any location in the laminate are expressed as linear combinations of the elements of the vector K. In particular, the transform $U_1(4h,k,s)$ of the normal displacement at the upper surface $x_1 = 4h$ has the form,

$$U_1(4h,k,s) = \frac{N(k,s)}{detM(k,s)}G(s), \tag{3}$$

where $N(k,s)$ is a known function of the transform parameters. The formal solution for the upper surface normal displacement is given by the inverse of the double transform,

$$u_1(4h,x,t) = \frac{1}{4\pi^2 i}\int_{-\infty}^{\infty}\int_{\gamma-i\infty}^{\gamma+i\infty}\frac{N(k,s)}{detM(k,s)}G(s)e^{st}e^{ikx}dsdk. \tag{4}$$

The integral with respect to s can be evaluated in terms of the residues of the integrand at the zeros of the function $detM(k,s)$ in the left hand plane. The equation,

$$detM(k,i\omega) = 0, \tag{5}$$

is the generalised Rayleigh-Lamb dispersion equation relating the angular frequency ω to the wave number k for plane harmonic waves propagating in the laminate. This equation has an infinite number of pairs of roots $\omega = \pm\omega_j(k)$, $j = 1, 2, \ldots$. Each curve $\omega = \omega_j(k)$ corresponds to one branch of the dispersion equation and in terms of these roots equation (4) becomes

$$u_1(4h, x, t) = \frac{1}{2\pi}\int_{-\infty}^{\infty} dk \sum_{j=1}^{\infty} \left\{ R(k,s)G(s)e^{i(kx-ist)} \right\}_{s=\pm i\omega_j(k)}. \tag{6}$$

Here $R(k,s)G(s)$ is the residue of the integrand, where $R(k,s)$ is given by

$$R(k,s) = \frac{N(k,s)}{d(detM)/ds} \tag{7}$$

and it may be shown to be an odd function of s.

For the step function input $G(s) = 1/s$ and the transform equation (6) may be written as

$$u_1(4h, x, t) = \frac{i}{\pi}\sum_{j=1}^{\infty}\int_{-\infty}^{\infty} R_j(k)\frac{[1-\cos\omega_j(k)t]}{\omega_j(k)}e^{ikx}dk, \tag{8}$$

where

$$R_j(k) = [R(k,s)]_{s=i\omega_j(k)} = -[R(k,s)]_{s=-i\omega_j(k)}. \tag{9}$$

It may further be shown that $R_j(k)$ is an even function of k so that equation (8) reduces to

$$u_1(4h, x, t) = \frac{2i}{\pi}\sum_{j=1}^{\infty}\int_{0}^{\infty} R_j(k)\frac{[1-\cos\omega_j(k)t]}{\omega_j(k)}\cos kx dk. \tag{10}$$

RESULTS

The material constants employed in order to obtain numerical results are detailed in [1]. The results are presented as graphs showing the time history of the upper surface normal displacement due to a crack opening line dislocation acting at one of the interfaces. This normal displacement is given by equation (10) which involves an infinite sum of infinite integrals and in order to perform the numerical evaluation the range of integration is restricted to a finite interval $(0, \hat{k})$ and the summation is restricted to a finite number of branches of the dispersion curve. In performing the evaluations, it is convenient to nondimensionalise the distance x and the time t by introducing $X = x/h$ and $T = ct/h$, where c is a typical wave speed. This results in nondimensional transform parameters $K = kh$ and $\Omega = \omega h/c$ and the numerical evaluations have been carried out for $\hat{K} = 10$, using a total of twenty branches of the dispersion curves, ten for each of the symmetric and the antisymmetric motions. In these calculations $c = 2.97$km/s and $h = 0.125$mm, which gives $\hat{k} = 8 \times 10^4 \mathrm{m}^{-1}$ and a plate thickness of 1mm. The nondimensional angular frequency ranges from zero to a maximum of $\Omega \approx 7.9$, corresponding to a frequency of about 30MHz. Table 1 lists the speeds v_1, v_2, v_3, of the three body waves that can propagate in the plane of the fibers in the directions making angles of $\gamma = 0^0$, 45^0, and 90^0 with the fibers. The table also gives the Rayleigh wave speed v_R in each of these three directions for surface waves propagating on a half space of the material.

Table 1. Body and surface wave speeds in fiber composite material.

γ	v_1(mm/μs)	v_2(mm/μs)	v_3(mm/μs)	v_R(mm/μs)
0^0	10.09	2.12	2.12	2.09
45^0	7.32	2.50	1.83	1.50
90^0	2.97	2.12	1.49	1.39

Figure 1 consists of seven curves, each curve showing the scaled upper surface normal displacement as a function of the nondimensional time. The curves, which are numbered 1-7, correspond to line sources acting in the plane $x_3 = 0$ and located at the interfaces $x_1 = 3h,\ 2h,\ h,\ 0,\ -h,\ -2h,$ and $-3h$, respectively. Each source gives rise to straight crested waves travelling in the direction Ox_3 and the receiver location is at a distance of $160h$ (20 plate thicknesses) from the plane of the sources along the propagation direction, which is the fiber direction in the surface layer. Figure 2 also consists of seven curves which represent the response to sources lying in the plane $x_2 = 0$ and located at each of the seven interfaces. In this case the straight crested waves travel at right angles to the fibers in the surface along the direction Ox_2 and the response is plotted for a surface receiver located at a distance of 20 plate thicknesses along this direction.

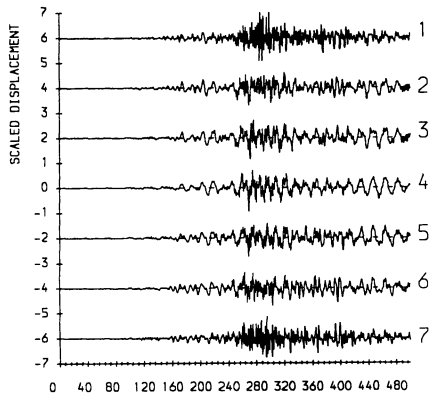

Figure 1. Top surface normal displacement at $x = 160h$ due to a crack opening line dislocation for $\gamma = 0^0$. Source located at 1 $x_1 = 3h$, 2 $x_1 = 2h$, 3 $x_1 = h$, 4 $x_1 = 0$, 5 $x_1 = -h$, 6 $x_1 = -2h$, 7 $x_1 = -3h$.

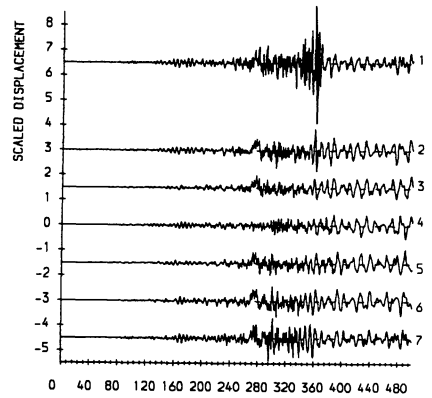

Figure 2. Top surface normal displacement at $x = 160h$ due to a crack opening line dislocation for $\gamma = 90^0$. Source located at 1 $x_1 = 3h$, 2 $x_1 = 2h$, 3 $x_1 = h$, 4 $x_1 = 0$, 5 $x_1 = -h$, 6 $x_1 = -2h$, 7 $x_1 = -3h$.

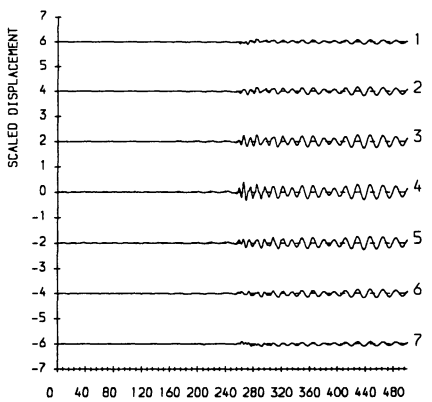

Figure 3. Contributions to Figure 1 from fundamental modes of symmetric and antisymmetric Rayleigh-Lamb waves.

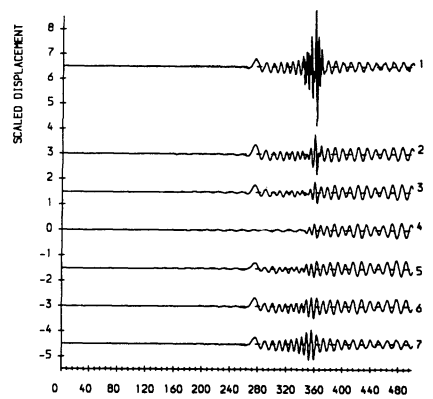

Figure 4. Contributions to Figure 2 from fundamental modes of symmetric and antisymmetric Rayleigh-Lamb waves.

The graphs shown in Figures 1 and 2 are obtained by combining contributions to the expression (10) from each of the first ten modes of the symmetric and the antisymmetric solutions. The symmetric solutions are derived for any source location by placing a source of one half the original strength at that location and an equal and opposite source at the mirror image location relative to the mid-plane. For the antisymmetric solution a source of one half the original strength is placed at the source location and an equal source is placed at the mirror image. In this way it is only necessary to solve for sources at the top three interfaces and at the mid-plane, in order to obtain the seven curves shown in Figures 1 and 2. Thus, the top three curves are obtained by adding together the symmetric and antisymmetric solutions, the bottom three by subtracting the antisymmetric solution from the symmetric solution, whilst the middle curve is derived from the symmetric modes only. Figures 3 - 10 show the results of combining some of the corresponding modes of the symmetric and antisymmetric solutions in this way to obtain the individual modal contributions for each of the seven sources. Figures 3 and 4 show the contributions arising from the fundamental modes (modes 1) for waves propagating at angles 0^0 and 90^0 to the fiber direction in the outer layer, respectively. Figures 5 and 6 are the contributions from mode 2, Figures 7 and 8 are for mode 7 and Figures 9 and 10 are the contributions from mode 10.

DISCUSSION

All the curves in Figures 1 and 2 show the earliest arrivals at a nondimensional time of $T \approx 100$, corresponding to a travel time of $t \approx 4.2\mu$s and a wave speed of 4.75mm/μs. This very low amplitude low frequency motion is followed by a larger amplitude low frequency arrival at $T \approx 160$, $t \approx 6.7\mu$s at a speed of 2.97mm/μs and this in turn is followed by a high frequency disturbance of larger amplitude with arrival time $T \approx 240$, $t \approx 10.1\mu$s and wave speed 1.98mm/μs. The maximum amplitudes of all the curves in Figure 1 are roughly equal to each other, whereas the top curve in Figure 2 has a maximum amplitude of the order of 2.5 times those of Figure 1 and of the other six curves in Figure 2. This large amplitude disturbance has an arrival time of $t \approx 15\mu$s corresponding to a wave speed of 1.32mm/μs which is close to that of the surface wave propagating at right angles to the fiber direction. The existence of a surface wave disturbance at this orientation of the load line and its nonexistence for waves propagating parallel to the surface fiber direction (Figure 1), is in accord with earlier results [3] and it is associated with the behaviour of the dipersion curves in the short wavelength limit. It is evident from Figure 1 that the amplitude of the surface disturbance is not significantly affected by the location of the source whereas in Figure 2, the sources at the midplane (curve 4) and at the interfaces closest to the midplane (curves 3 and 5) give rise to smaller amplitude surface disturbances than the sources at the outer interfaces.

Figures 3 and 4 show the contributions of the fundamental modes to the overall response due to each of the seven sources. Figure 3 relates to propagation along Ox_3 and Figure 4 to propagation along Ox_2. Curve 1 of Figure 4 shows that the large amplitude disturbance in curve 1 of Figure 2 arises from the fundamental mode and this accords with the fact that in this case the short wave limiting phase velocity of the fundamental modes is that of the Rayleigh surface wave. For propagation along Ox_3, the limiting phase velocity of the fundamental modes is the velocity of shear waves in the core and it is for this reason that there is no surface wave disturbance to be seen in Figure 3. Figures 5 and 6 show the contributions from the second modes. These curves have smaller amplitudes than those in Figures 3 and 4 but they show the presence of some high frequency motion in addition to a low frequency disturbance oscillation such as is seen in Figures 3 and 4. The contributions from modes 3 - 6 are generally smaller than those from mode 2 and the most significant higher harmonic contributions are those from mode 7 which are shown in Figures 7 and 8. It is clear from these that curves 1 and 7 of Figure 7 make a substantial contribution to the overall response to be seen in the corresponding curves of Figure 1. Whilst this is not the

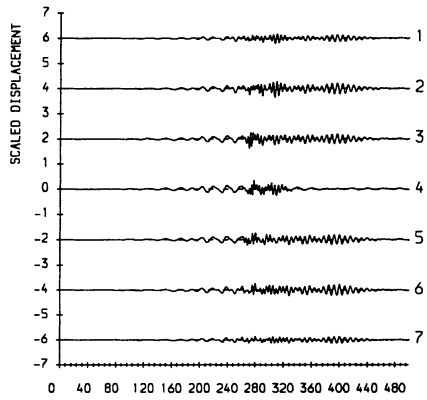

Figure 5. As Figure 3 but for second modes.

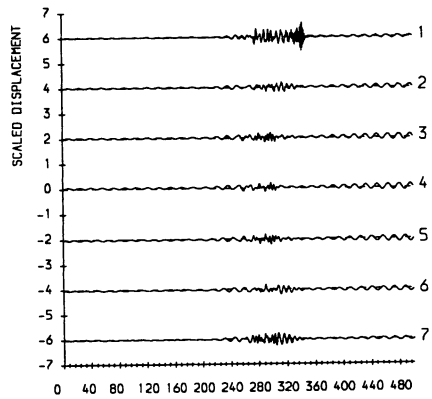

Figure 6. As Figure 4 but for second modes.

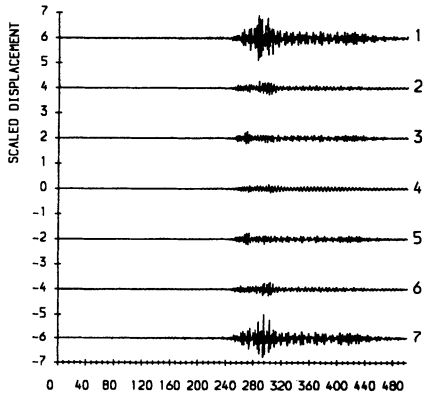

Figure 7. As Figure 3 but for modes 7.

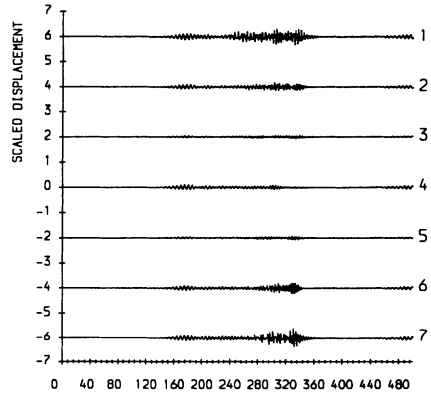

Figure 8. As Figure 4 but for modes 7.

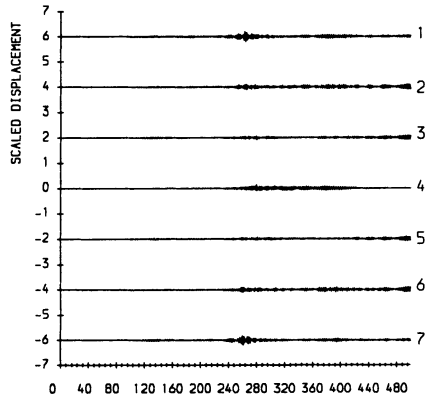

Figure 9. As Figure 3 but for modes 10.

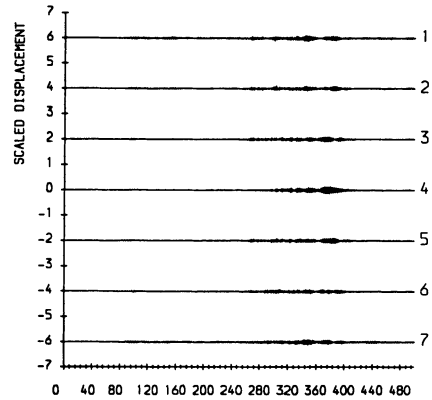

Figure 10. As Figure 4 but for modes 10.

case for curves 2-6 it is nevertheless clear that the contributions from Figures 3, 5 and 7 together are sufficient to give a good approximation to the curves shown in Figure 1. The contributions from Figure 8 to the overall response shown in Figure 2 are not as significant as the previous case since for propagation in this direction the fundamental modes play a large part in the disturbance. Nevertheless, the combined response of Figures 4, 6 and 8 will here also give a satisfactory approximation to the overall responses of Figure 2. Figures 9 and 10 show the contributions from mode 10. They show small amplitude high frequency disturbances whose effect on the overall response are not negligible.

An alternative approach to that employed here has been adopted by Lih and Mal [4] who model the plate by means of classical laminate theory with a shear correction. They show that for ramp step functions with relatively slow rise times this shear corrected classical laminate model yields results in good agreement with the full solution method used here. The shear corrected theory replicates the fundamental mode of the Rayleigh-Lamb solution but it does not include the higher harmonics. The results presented here show that, for the step function source, the contributions to the overall response in the far field from the higher modes of the Rayleigh-Lamb equations can be significant. These higher modes give rise to high frequency disturbances and the sharp step function involves contributions at all frequencies. For a smoothly rising ramp step function with a rise time of the order of $0.5\mu s$ or greater, the contributions from frequencies greater than some 3MHz will be negligible. In these circumstances the shear corrected laminate theory used by Lih and Mal [4] can be expected to give adequate results.

ACKNOWLEDGEMENTS

This work was supported in part by the Engineering and Physical Sciences Research Council under research grant number GR/H90223.

REFERENCES

1. E.Rhian Green, in *Review of Progress in QNDE*, this Vol.
2. E.Rhian Green, Composites Engineering, 3, 437 (1993).
3. E.Rhian Green, Composites Engineering, 5, 1453 (1995).
4. S-S.Lih and A.K.Mal, Composites, 27, 633 (1996).